

The transition from conservative to dissipative flows in class-B laser model with fold-Hopf bifurcation and coexisting attractors

Yue Li(李月), Zengqiang Chen(陈增强), Mingfeng Yuan(袁明峰), and Shijian Cang(仓诗建)
Citation: Chin. Phys. B, 2022, 31 (**6**): 060503. DOI: 10.1088/1674-1056/ac43a2
Journal homepage: http://cpb.iphy.ac.cn; http://iopscience.iop.org/cpb

What follows is a list of articles you may be interested in

Design and FPGA implementation of a memristor-based multi-scroll hyperchaotic system

Sheng-Hao Jia(贾生浩), Yu-Xia Li(李玉霞), Qing-Yu Shi(石擎宇), and Xia Huang(黄霞)
Chin. Phys. B, 2022, 31 (**7**): 070505. DOI: 10.1088/1674-1056/ac4a71

The transition from conservative to dissipative flows in class-B laser model with fold-Hopf bifurcation and coexisting attractors

Yue Li(李月), Zengqiang Chen(陈增强), Mingfeng Yuan(袁明峰), and Shijian Cang(仓诗建)
Chin. Phys. B, 2022, 31 (**6**): 060503. DOI: 10.1088/1674-1056/ac43a2

Inferring interactions of time-delayed dynamic networks by random state variable resetting

Changbao Deng(邓长宝), Weinuo Jiang(蒋未诺), and Shihong Wang(王世红)
Chin. Phys. B, 2022, 31 (**3**): 030502. DOI: 10.1088/1674-1056/ac1e12

Nonlinear dynamics analysis of cluster-shaped conservative flows generated from a generalized thermostatted system

Yue Li(李月), Zengqiang Chen(陈增强), Zenghui Wang(王增会), and Shijian Cang(仓诗建)
Chin. Phys. B, 2022, 31 (**1**): 010501. DOI: 10.1088/1674-1056/ac0a61

Dynamics analysis of a 5-dimensional hyperchaotic system with conservative flows under perturbation

Xuenan Peng(彭雪楠), Yicheng Zeng(曾以成), and Qi Xie(谢奇)
Chin. Phys. B, 2021, 30 (**10**): 100502. DOI: 10.1088/1674-1056/abea9a

---

SPECIAL TOPIC — Interdisciplinary physics: Complex network dynamics and emerging technology

The transition from conservative to dissipative flows in class-B laser model with fold-Hopf bifurcation and coexisting attractors

Yue Li(李月)[1], Zengqiang Chen(陈增强)[1,†], Mingfeng Yuan(袁明峰)[2], and Shijian Cang(仓诗建)[3,‡]

[1] *College of Artificial Intelligence, Nankai University, Tianjin* 300350, *China*
[2] *Department of Earth and Space Science and Engineering, York University,* 4700 *Keele St, Toronto M3J* 1*P3, Canada*
[3] *Department of Product Design, Tianjin University of Science and Technology, Tianjin* 300222, *China*

(Received 22 September 2021; revised manuscript received 21 November 2021; accepted manuscript online 16 December 2021)

Dynamical behaviors of a class-B laser system with dissipative strength are analyzed for a model in which the polarization is adiabatically eliminated. The results show that the injected signal has an important effect on the dynamical behaviors of the system. When the injected signal is zero, the dissipative term of the class-B laser system is balanced with external interference, and the quasi-periodic flows with conservative phase volume appear. And when the injected signal is not zero, the stable state in the system is broken, and the attractors (period, quasi-period, and chaos) with contractive phase volume are generated. The numerical simulation finds that the system has not only one attractor, but also coexisting phenomena (period and period, period and quasi-period) in special cases. When the injected signal passes the critical value, the class-B laser system has a fold-Hopf bifurcation and exists torus "blow-up" phenomenon, which will be proved by theoretical analysis and numerical simulation.

Keywords: conservative flows, dissipative attractors, coexisting phenomena, fold-Hopf bifurcation, class-B laser chaotic system

PACS: 05.45.–a

DOI: 10.1088/1674-1056/ac43a2

1. Introduction

According to the conservative property of phase volume, the phase trajectories of the system can be divided into conservative flows (phase volume is conservative) and dissipative flows (phase volume is contractive). Since Lorenz proposed the Lorenz system in 1963,[1] dissipative systems have been extensively studied.[2–7] In recent years, with the further exploration of chaos theory, conservative flows have gradually become a research hotspot in the nonlinear field. For example, based on the generalized Hamiltonian system theory, the Cang team proposed a class of multi-cluster conservative chaotic systems (3D and 4D) with complex topological structures,[8–10] and the Dong team proposed some high-dimensional Hamiltonian conservative chaotic systems with multistability and designed a pseudo-random number generator.[11] In addition, the Qi team proposed some Hamiltonian conservative chaotic systems based on 4D Euler equations, and analyzed the reason why these systems can produce conservative chaos from the perspective of energy.[12,13] From the above introduction, it can be seen that the phase volume of the flows generated by the existing system is mostly single (conservative or dissipative). Based on this, this paper studies a class-B laser system, which can realize the transition from conservative flows to dissipative flows.

A laser is a device that emits light through a process of optical amplification or oscillation based on the stimulated emission of electromagnetic radiation.[14] In the 1980s, some scholars successively studied the class-B laser system with injected signal, and discovered chaos, Hopf bifurcation, and other dynamical behaviors.[15–17] In recent years, there are some scholars studying this system. Such the paper which analyzed the dynamic characteristics of a class-B laser model, it also found chaos by variable delayed optoelectronic feedback;[18] Wang *et al.* studied the Hopf bifurcation and double Hopf bifurcation phenomena of the class-B laser system;[14] Similarly, Li also investigated the double Hopf bifurcation of a class-B laser system.[19] However, the current researches on the class-B laser system are still subject to further exploration of chaos and Hopf bifurcation phenomena, and its internal dynamic characteristics had not been discovered yet. Therefore, this paper conducts deeper research on the class-B laser system. The contributions of this paper are as follows:

(i) Even if the system structure is not changed, the class-B laser system realizes the transition from conservative flows to dissipative attractors (period, quasi-period and chaos);

(ii) When the injected signal is not zero, there are two coexisting phenomena (period and period, period and quasi-period) in the class-B laser system;

(iii) The class-B laser system has fold-Hopf bifurcation

†Corresponding author. E-mail: chenzq@nankai.edu.cn
‡Corresponding author. E-mail: sj.cang@gmail.com

© 2022 Chinese Physical Society and IOP Publishing Ltd

which is proved by the theoretical analysis and numerical simulation.

The rest of this paper is divided into six sections as follows. Section 2 introduces a class-B laser system and transforms this system into the generalized Hamiltonian system form. Section 3 analyzes the equilibria characteristics of the class-B laser system. In Section 4, the transition of the class-B laser system from conservative flows to dissipative attractors is analyzed. Section 5 introduces the coexisting phenomena in the system. The theoretical derivation and numerical simulation of the fold-Hopf bifurcation in the class-B laser system are introduced in Section 6. Finally, some conclusions are drawn in Section 7.

2. System description

By correcting the Maxwell–Bloch equations of a single-mode, homogeneously broadened ring laser with external signal, and separating the field variable into the amplitude and phase with respect to the external field, one gets a class-B laser system with injected signal:[17,20,21]

$$\begin{cases} \dot{r} = zr + k\cos\varphi, \\ \dot{\varphi} = -w - \dfrac{k}{r}\sin\varphi, \\ \dot{z} = D - r^2 - a\left(1 + gr^2\right)z, \end{cases} \tag{1}$$

where r represents the cavity field amplitude, φ is measured with respect to a frame rotating at the frequency of the external laser (for simplicity, phase φ equal to the atomic frequency), z represents the population inversion. The parameters w, a, k are the cavity mistuning, the square root of the ratio, and the Rabi frequency of the external field normalized to the new time scale, respectively. D is the pump parameter referred to the threshold value. and finally, g is the multiplicative factor. Using Cartesian coordinates expresses system (1), and letting $D = 1, g = 1$, we can get

$$\begin{cases} \dot{x} = xz + wy + k, \\ \dot{y} = yz - wx, \\ \dot{z} = (1 - az)\left(1 - x^2 - y^2\right). \end{cases} \tag{2}$$

According to the generalized Hamiltonian system form[8–13,22]

$$\dot{X} = A(X)\nabla H(X) - \Lambda(X)\nabla H(X) + U, \tag{3}$$

where X is the state vector; $A(X)$ is the skew-symmetric state matrix satisfying $A(X) = -A(X)^{\mathrm{T}}$; $\Lambda(X)$ is an indefinite matrix satisfying $\Lambda(X) = -\Lambda(X)^{\mathrm{T}}$; $\nabla H(X)$ is the gradient vector of Hamiltonian $H(X)$; and U is a matrix composed of column vectors that represents the exchange energy between the system and the outside world. In terms of energy, $A(X)\nabla H(X)$, $\Lambda(X)\nabla H(X)$ and U represent the conservative term, the dissipative term, and the external interference of the system (3). Therefore, according to Eq. (3), the system (2) can be expressed as

$$\begin{pmatrix} \dot{x} \\ \dot{y} \\ \dot{z} \end{pmatrix} = \begin{pmatrix} 0 & w & x \\ -w & 0 & y \\ -x & -y & 0 \end{pmatrix} \begin{pmatrix} x \\ y \\ z \end{pmatrix} - \begin{pmatrix} 0 & 0 & 0 \\ 0 & 0 & 0 \\ 0 & 0 & a(1 - x^2 - y^2) \end{pmatrix} \begin{pmatrix} x \\ y \\ z \end{pmatrix} + \begin{pmatrix} k \\ 0 \\ 1 \end{pmatrix}. \tag{4}$$

Obviously, the parameter a determines the dissipative strength in system (2), this paper will discuss the dynamical characteristics of system (2) at $a \neq 0$.

3. Equilibrium analysis

Let $\dot{x} = 0, \dot{y} = 0, \dot{z} = 0$, the equilibrium points for system (2) are as follows:

(I) When $k \in (-w, w)$, system (2) has the only equilibrium

$$S_1 = \left(-\frac{ak}{a^2w^2 + 1}, -\frac{a^2wk}{a^2w^2 + 1}, \frac{1}{a}\right), \tag{5}$$

for all values of w, a, and k with the Jacobian matrix

$$J_{S_1} = \begin{pmatrix} \dfrac{1}{a} & w & -\dfrac{ak}{a^2w^2 + 1} \\ -w & \dfrac{1}{a} & -\dfrac{a^2kw}{a^2w^2 + 1} \\ 0 & 0 & \dfrac{a\left(a^2k^2 - a^2w^2 - 1\right)}{a^2w^2 + 1} \end{pmatrix}$$

having eigenvalues

$$\begin{cases} \lambda_1 = \dfrac{a\left(a^2k^2 - a^2w^2 - 1\right)}{a^2w^2 + 1}, \\ \lambda_{2,3} = \dfrac{1}{a} \pm w\mathrm{i}, \end{cases}$$

which indicates that S_1 is unstable if $a \in \mathbb{R}^+$.

(II) When $k = w$ or $k = -w$, system (2) adds an equilibrium point $S_R = (0, -1, 0)$ or $S_L = (0, 1, 0)$. In other words, there are two equilibrium points $S_{1,R}$ or $S_{1,L}$ in system (2) at this time.

(III) When $k \in (-\infty, -w) \cup (w, +\infty)$, S_R or S_L disappears, but there are two other equilibria in system (2):

$$\begin{cases} S_2 = \left(\dfrac{\sqrt{k^2 - w^2}}{k}, -\dfrac{w}{k}, -\sqrt{k^2 - w^2}\right), \\ S_3 = \left(-\dfrac{\sqrt{k^2 - w^2}}{k}, -\dfrac{w}{k}, \sqrt{k^2 - w^2}\right). \end{cases} \tag{6}$$

At this time, the system (2) has three equilibrium points $S_{1,2,3}$.

It is difficult to produce the analytical solutions of the eigenvalues by substituting $S_{2,3}$ into their corresponding Jacobian matrixes. For simplicity, let $a = 1$ and $w = 1$, then one can obtain the numerical results of the eigenvalues at $S_{1,2,3}$ when k varies, as shown in Fig. 1. As can be seen from the figure, when the parameter k passes through the critical values $w = \pm 1$, the equilibrium points $S_{2,3}$ will disappear or appear, which indicates that S_{L} and S_{R} are the potential bifurcation points. Since the equilibria are symmetrical about $k = 0$, this paper can only consider the dynamics of the system (2) at

$k \geqslant 0$.

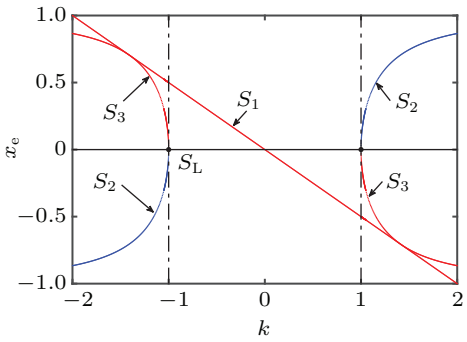


Fig. 1. Plot of the distribution of the equilibria of the system (2) with respect to k varying in the interval $[-2,2]$, and their corresponding stability when $a=1$ and $w=1$. The blue and red curves are the marks of the stable and unstable equilibria, respectively. S_L and S_R denote the bifurcation points.

4. Transition from conservation to dissipation

Keeping $a=1$ and $w=1$, when $k=0$, the phase trajectories of system (2) starting from different initial conditions $J_0=(0.2,0.1,0.1), J_1=(0.3,0.1,0.1),\ldots,J_6=(0.8,0.1,0.1)$ form the nested quasi-periodic motions, their corresponding Poincaré section is shown in Fig. 2(a). The closed curves with different colors in Fig. 2(a) further indicate that there exist the coexistence of multiple quasi-periods in system (2) when $k=0$. In addition, the Lyapunov exponents $(LE_1,LE_2,LE_3)=(0,0,0)$ indicate that these quasi-periodic motion are conservative flows. In the nonlinear system, since the dissipative term is difficult to keep balance with the conservative term and the external interference, it is difficult to find the conservative flows in the system containing the dissipative term. By calculation, the reason why the system (2) can produce conservative flows is that when $k=0$, the dissipative term in system (2) is always in balance with the external interference, hence the nested closed curves in Fig. 2(a) appear. And when $k\neq 0$, the stable state in system (2) is destroyed due to the interference of the parameter k, that is, the closed curves in Fig. 2(a) will no longer exist. Figure 2(b) shows the Poincaré section generated by system (2) at $k=0.01$, as we can see from the figure, the seemingly closed rings are actually some irregular discrete points, these show that when $k=0.01$, the quasi-periodic motions are disturbed and turn into chaotic motion.

With the continuous increase of the value of k, the dissipative characteristics of system (2) are also becoming more and more obvious. Figure 3 shows the Lyapunov exponents of system (2) while $k\in[0.2,0.7]$. It can be seen from the figure that when k takes different values, the system (2) has dynamical behaviors with different characteristics. For example, when $k=0.4$, the Lyapunov exponents $(LE_1,LE_2,LE_3)=(0,-0.13,-0.13)$ indicate that there is a periodic orbit in system (2); when $k=0.55$, the Lyapunov exponents $(LE_1,LE_2,LE_3)=(0,0,-0.14)$ indicate that system (2) has quasi-periodic motion; and the Lyapunov exponents $(LE_1,LE_2,LE_3)=(0.14,0,-0.24)$ when $k=0.67$ indicate that the system (2) has chaotic motion. These phenomena are shown in Fig. 4.

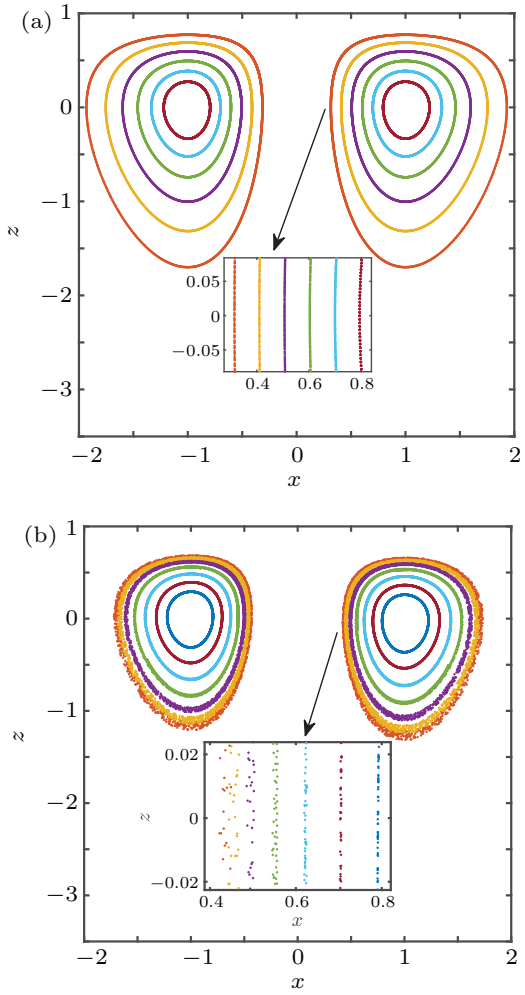


Fig. 2. When the parameters $a=1$ and $w=1$, Poincaré sections of the system (2) on the x–z plane ($y=0$) with different initial conditions $J_{0,1,\ldots,6}$: (a) $k=0$; (b) $k=0.01$.

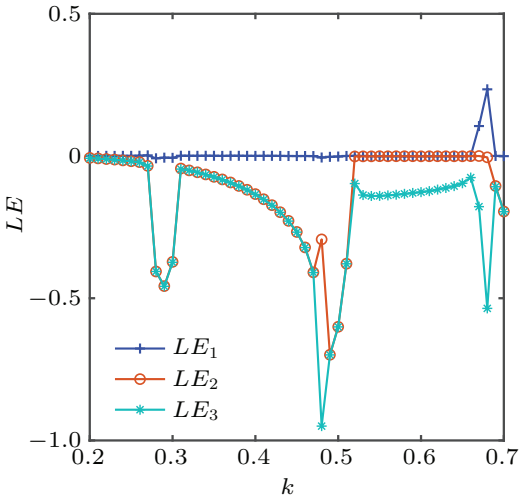


Fig. 3. When the parameters $a=1$, $w=1$, Lyapunov exponents of the system (2) from the initial conditions $I_0=(0.1,0.1,0.1)$ with $k\in[0.2,0.7]$.

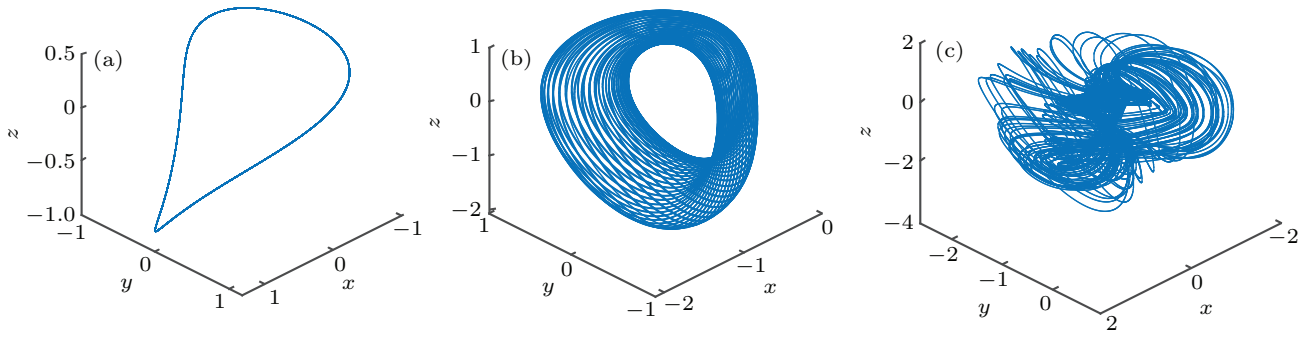


Fig. 4. When the parameters $a = 1$, $w = 1$, 3D phase portraits the system (2) from the initial conditions $I_0 = (0.1, 0.1, 0.1)$ with different k: (a) $k = 0.4$; (b) $k = 0.55$; (c) $k = 0.67$.

5. Coexisting phenomena

According to the Section 4, when $a = 1$, $w = 1$ and $k \neq 0$, no matter what motion (period, quasi-period, or chaos) is produced by system (2), its phase volume is always contractive. That is to say, the phase trajectories in Fig. 4 are independent attractors. However, through numerical simulation, it is finds that system (2) has not only one attractor, but also two attractors in special cases, that is, coexisting attractors.

Figure 5(a) shows the two coexisting periodic attractors P_1 and P_2 which exist in the system (2) when $k = 0.3$, which are generated by the initial values $P_1 = (0.8, 0.5, 0.5)$ and $P_2 = (0.5, 0.5, 0.5)$, respectively. In addition, when $k = 0.89$, the system (2) also has the coexisting phenomenon. By choosing the initial conditions $N_1 = (0.5, -0.6, 0.5)$ and $N_2 = (0.5, 0.5, 0.5)$, and they generate the quasi-periodic motion N_1 and the periodic motion N_2 as shown in Fig. 5(b), respectively.

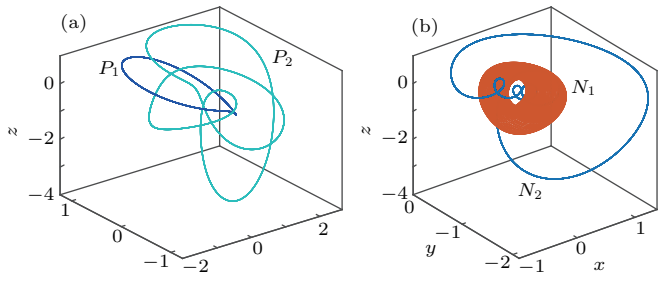


Fig. 5. The 3D phase portraits of system (2) with the parameters $a = 1, w = 1$: (a) parameter $k = 0.3$ and the initial values $P_1 = (0.8, 0.5, 0.5)$ and $P_2 = (0.5, 0.5, 0.5)$; (b) parameter $k = 0.89$ and the initial values $N_1 = (0.5, -0.6, 0.5)$ and $N_2 = (0.5, 0.5, 0.5)$.

Under given parameter conditions, according to whether the basin of attraction of attractor contains the equilibrium point in phase space, attractor can be divided into self-excited attractor or hidden attractor.[23] The basin of attraction of self-excited attractor contains the equilibrium point, while the basin of attraction of hidden attractor does not contains the equilibrium point. When $a = 1$, $w = 1$ and $k \in (-w, w)$, according to Eq. (5), we have a single equilibrium point

$$S_1 = \left(-\frac{k}{2}, -\frac{k}{2}, 1\right).$$

Further, when $k = 0.3$ or $k = 0.89$, one can get $\tilde{S}_1 = (-0.15, -0.15, 1)$ or $\hat{S}_1 = (-0.445, -0.445, 1)$.

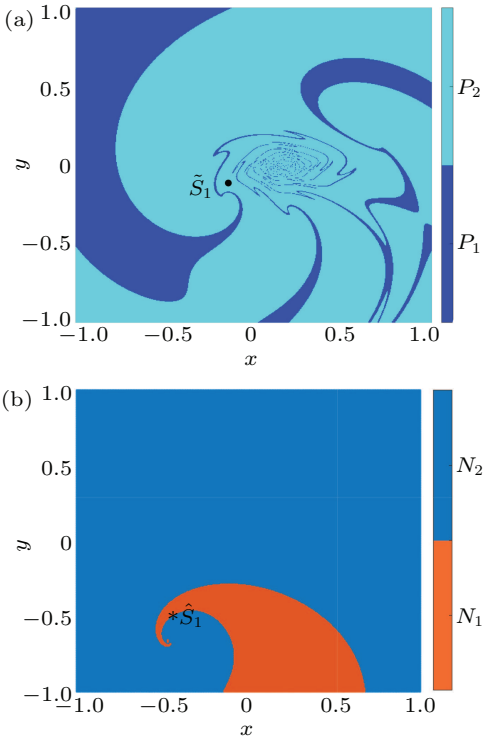


Fig. 6. Two colored basins of attraction of system (2) at $z = 0.5$ on the x–y plane; (a) $k = 0.3$; (b) $k = 0.89$.

In order to determine the type of attractors shown in Fig. 5, figures 6(a) and 6(b) show the basin of attraction of system (2) when $k = 0.3$ and $k = 0.89$, respectively. In Fig. 6(a), the dark blue area represents the basin of attraction of periodic motion P_1 in Fig. 5(a), the light blue area represents the basin of attraction of periodic motion P_2, and the equilibrium point $\tilde{S}_1$ is represented by "•". It can be seen from the figure that equilibrium point $\tilde{S}_1$ is located in the light blue area, which indicates that the periodic motion P_2 in Fig. 5(a) is a self-excited attractor, and the periodic motion P_1 is a hidden attractor. Further, in Fig. 6(b), the red area represents the basin of attraction of quasi-periodic motion N_1 in Fig. 5(b), the blue area represents the basin of attraction of periodic motion N_2, and the equilibrium point $\hat{S}_1$ is represented by "$*$". Obviously, the different colors do not intersect each other, but this is enough to determine the type of the two attractors N_1 and N_2 in Fig. 6(b).

To further determine the type of attractors N_1 and N_2, one keeps the parameters a and w unchanged, and chooses an initial values $X_0 = (-0.445, -0.445, 0.9999)$ that are very close to the equilibrium points $\hat{S}_1$. When $k = 0.89$, the study finds that the motion X_0 (Fig. 7) starting from the initial value X_0 similar to that of the periodic motion N_2 in Fig. 5(b). This shows that the basin of attraction of the periodic motion N_2 intersects with open neighborhood of the equilibrium point $\hat{S}_1$, which in turn indicates that the periodic orbit N_2 is a self-excited attractor, and the quasi-periodic motion N_1 is a hidden attractor.

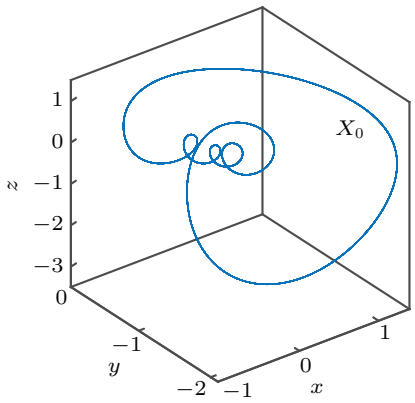


Fig. 7. The 3D phase portraits of system (2) with the parameters $a = 1$, $w = 1$, $k = 0.89$ and the initial conditions $X_0 = (-0.445, -0.445, 0.9999)$.

6. Fold-Hopf bifurcation

6.1. Derivation of the normal form

The fold-Hopf bifurcation is a bifurcation of an equilibrium point in a two-parameter family of autonomous ODEs at which the critical equilibrium has a zero eigenvalue and a pair of purely imaginary eigenvalues.[24] Consider an autonomous system of ordinary differential equations (ODEs):

$$\dot{X} = f(X, \alpha), \tag{7}$$

where $X = (x, y, z)^{\mathrm{T}} \in \mathbb{R}^3$, $\alpha = (\omega, k)^{\mathrm{T}} \in \mathbb{R}^2$ and f is a sufficiently smooth function of (X, α). Suppose that at $\alpha = \alpha_0 = 0$ the system has an equilibrium $X_0 = 0$ with one zero eigenvalue $\lambda_1 = 0$ and a pair of purely imaginary eigenvalues $\lambda_{2,3} = \pm \mathrm{i}\omega_0$ with $\omega_0 > 0$, and then the Taylor expansion of $f(X, \alpha_0)$ near X_0 can be written as

$$\begin{aligned} f(X, \alpha_0) \ =& \ AX + \frac{1}{2}B(X,X) \\ &+ \frac{1}{6}C(X,X,X) + O\left(\|X\|^4\right), \end{aligned} \tag{8}$$

where A is the Jacobian matrix of Eq. (7) at X_0, $B(X,X)$ and $C(X,X,X)$ are bilinear and trilinear functions, respectively. In coordinates, one can obtain

$$B_i(X,X) = \sum_{j,k=1}^{3} \frac{\partial^2 f_i(\xi)}{\partial \xi_j \partial \xi_k}\bigg|_{\xi=0} X_j X_k, \tag{9}$$

$$C_i(X,X,X) = \sum_{j,k,l=1}^{3} \frac{\partial^3 f_i(\xi)}{\partial \xi_j \partial \xi_k \partial \xi_l}\bigg|_{\xi=0} X_j X_k X_l, \tag{10}$$

where $i = 1, 2, 3$.

Introduce two eigenvectors: $q_0 \in \mathbb{R}^3$ and $q_1 \in \mathbb{C}^3$, satisfying

$$Aq_0 = 0 \ \text{ and } \ Aq_1 = \mathrm{i}\omega_0 q_1,$$

and two adjoint eigenvectors: $p_0 \in \mathbb{R}^3$ and $p_1 \in \mathbb{C}^3$, satisfying

$$A^{\mathrm{T}} p_0 = 0 \ \text{ and } \ A^{\mathrm{T}} p_1 = -\mathrm{i}\omega_0 p_1.$$

Normalize these eigenvectors such that

$$\langle p_0, q_0 \rangle = \langle p_1, q_1 \rangle = 1,$$

and the orthogonality properties must be hold:

$$\langle p_1, q_0 \rangle = \langle p_0, q_1 \rangle = 0.$$

Here, $\langle \cdot, \cdot \rangle$ denotes the standard scalar product in $\mathbb{C}^3$. Any vector $X \in \mathbb{R}^3$ can be uniquely expressed as

$$X = \zeta_0 q0 + \zeta_1 q_1 + \bar{\zeta}_1 \bar{q}_1, \tag{11}$$

where $\zeta_0 = \langle p_0, X \rangle \in \mathbb{R}^1$ and $\zeta_1 = \langle p_1, X \rangle \in \mathbb{C}^1$.

Lemma 1 (Gavrilov normal form) If the system (7) meets the following conditions:[25]

i) $G_{200} \neq 0$;

ii) $G_{011} \neq 0$;

iii) $E(0) \neq 0$.

Then system (7) is equivalent to the system

$$\begin{cases} \dot{\zeta}_0 = \delta(\alpha) + B(\alpha)\zeta_0^2 + C(\alpha)|\zeta_1|^2 + O\left(\|\zeta_0, \zeta_1, \bar{\zeta}_1\|^4\right), \\ \dot{\zeta}_1 = \Sigma(\alpha)\zeta_1 + D(\alpha)\zeta_0\zeta_1 + E(\alpha)\zeta_0^2\zeta_1 + O\left(\|\zeta_0, \zeta_1, \bar{\zeta}_1\|^4\right), \end{cases} \tag{12}$$

by a linear scaling of the variables ζ_0, ζ_1, and time t in system (12), one obtains

$$\begin{cases} \dot{\xi} = \beta_1 + \xi^2 + s|\zeta|^2 + O(\|(\xi, \zeta, \bar{\zeta})\|^4), \\ \dot{\zeta} = (\beta_2 + \mathrm{i}\omega_1)\zeta + (\theta + \mathrm{i}\vartheta)\xi\zeta + \xi^2\zeta + O(\|(\xi, \zeta, \bar{\zeta})\|^4), \end{cases} \tag{13}$$

where $\xi \in \mathbb{R}^1$ and $\zeta \in \mathbb{C}^1$ are new variables; β_1 and β_2 are new parameters; $\theta = \theta(0)$, $\vartheta = \vartheta(0)$, $\omega_1 = \omega_1(0)$ and

$$\begin{cases} s = \mathrm{sign}(B(0)C(0)) = \pm 1, \\ \theta(0) = \dfrac{\mathrm{Re}(H_{110})}{B(0)}. \end{cases} \tag{14}$$

Here, $B(0) = G_{200}, C(0) = G_{011}$, while

$$E(0) = \mathrm{Re}\left[H_{210}(0) + H_{110}(0)\Gamma - \Psi\right], \tag{15}$$

where

$$\begin{cases} \Gamma = \dfrac{\mathrm{Re}H_{021}(0)}{G_{011}(0)} - \dfrac{3G_{300}(0)}{2G_{200}(0)} + \dfrac{G_{111}(0)}{2G_{011}(0)}, \\ \Psi = \dfrac{H_{021}(0)\,G_{200}(0)}{G_{011}(0)}. \end{cases} \tag{16}$$

Compute all coefficients in formulas (15) and (16):

$$\begin{cases} G_{200} = \dfrac{1}{2}\langle p_0, B(q_0,q_0)\rangle, \\ H_{110} = \langle p_1, B(q_0,q_1)\rangle, \\ G_{011} = \langle p_0, B(q_1,\bar{q}_1)\rangle, \\ G_{300} = \dfrac{1}{6}\langle p_0, C(q_0,q_0,q_0) + 3B(q_0,h_{200})\rangle, \\ G_{111} = \langle p_0, C(q_0,q_1,\bar{q}_1) + B\left(q_1,\bar{h}_{110}\right) \\ \qquad + B(\bar{q}_1,h_{110}) + B(q_0,h_{011})\rangle, \\ H_{210} = \dfrac{1}{2}\langle p_1, C(q_0,q_0,q_1) \\ \qquad + 2B(q_0,h_{110}) + B(q_1,h_{200})\rangle, \\ H_{021} = \dfrac{1}{2}\langle p_1, C(q_1,q_1,\bar{q}_1) \\ \qquad + 2B(q_1,h_{011}) + B(\bar{q}_1,h_{020})\rangle, \end{cases} \tag{17}$$

where $h_{020} = (2\mathrm{i}\omega_0 I_3 - A)^{-1} B(q_1,q_1)$, with I_3 being a 3×3 identity matrix, while h_{200}, h_{011} and h_{110} can be solved by the (3+1)-dimensional bordered systems:

$$\begin{pmatrix} A & q_0 \\ p_0^{\mathrm{T}} & 0 \end{pmatrix}\begin{pmatrix} h_{200} \\ s \end{pmatrix} = \begin{pmatrix} -B(q_0,q_0) + \langle p_0, B(q_0,q_0)\rangle q_0 \\ 0 \end{pmatrix}, \tag{18}$$

$$\begin{pmatrix} A & q_0 \\ p_0^{\mathrm{T}} & 0 \end{pmatrix}\begin{pmatrix} h_{011} \\ s \end{pmatrix} = \begin{pmatrix} -B(q_1,\bar{q}_1) + \langle p_0, B(q_1,\bar{q}_1)\rangle q_0 \\ 0 \end{pmatrix}, \tag{19}$$

$$\begin{pmatrix} \mathrm{i}\omega_0 I_3 - A & q_1 \\ \bar{p}_1^{\mathrm{T}} & 0 \end{pmatrix}\begin{pmatrix} h_{110} \\ s \end{pmatrix} = \begin{pmatrix} B(q_0,q_1) - \langle p_1, B(q_0,q_1)\rangle q_1 \\ 0 \end{pmatrix}. \tag{20}$$

According to formula (14), the fold-Hopf bifurcation can be divided into three categories:

I) subcritical Hopf bifurcation and no tori ($s=1, \theta(0)>0$ or $s=-1, \theta(0)<0$);

II) subcritical and supercritical Hopf bifurcations and torus "heteroclinic destruction" ($s=1, \theta(0)<0$);

III) subcritical and supercritical Hopf bifurcations and torus "blow-up" ($s=-1, \theta(0)>0$).

6.2. Theoretical analysis

Proposition 1 When $a=1$ and $w=1$, and k passes through the critical values 1, system (2) undergoes a fold-Hopf bifurcation and presents a blow-up invariant tori near the fold-Hopf bifurcation point.

Proof When $a=1$, $w=1$ and $k=1$, system (2) has two equilibrium points:

$$\begin{cases} S_{\mathrm{R}} = (0,-1,0), \\ S_1 = (-1/2,-1/2,1), \end{cases} \tag{21}$$

the corresponding eigenvalues are

$$\left(\lambda_1^{S_{\mathrm{R}}}, \lambda_2^{S_{\mathrm{R}}}, \lambda_3^{S_{\mathrm{R}}}\right) = \left(0, -\mathrm{i}\sqrt{3}, \mathrm{i}\sqrt{3}\right),$$

and

$$\left(\lambda_1^{S_1}, \lambda_2^{S_1}, \lambda_3^{S_1}\right) = \left(-\frac{1}{2}, 1-\mathrm{i}, 1+\mathrm{i}\right).$$

In order to move the equilibrium point S_{R} to the origin, perform a linear coordinate shift on system (2) by introducing a new variable η:

$$\eta = y - 1. \tag{22}$$

Substituting Eq. (22) into Eq. (2) yields

$$\begin{cases} \dot{x} = \omega\eta + xz + k - \omega, \\ \dot{\eta} = -\omega x - z + \eta z, \\ \dot{z} = (az-1)\left(x^2 + \eta^2 - 2\eta\right). \end{cases} \tag{23}$$

For system (23) with $a=\omega=k=1$, there is an equilibrium $X_0=(0,0,0)$ with the eigenvalues: $\lambda_1=0$ and $\lambda_{2,3} = \pm\mathrm{i}\omega_0 = \pm\mathrm{i}\sqrt{3}$. So X_0 is a fold-Hopf bifurcation point and its corresponding Jacobian matrix A:

$$A = \begin{pmatrix} 0 & 1 & 0 \\ -1 & 0 & -1 \\ 0 & 2 & 0 \end{pmatrix}.$$

According to A, one can obtain these vectors in $\mathbb{C}^3$:

$$\begin{cases} q_0 = (1,0,-1)^{\mathrm{T}}, \\ q_1 = \left(-(\sqrt{3}/3)\mathrm{i}, 1, -(2\sqrt{3}/3)\mathrm{i}\right)^{\mathrm{T}}, \\ p_0 = (2/3, 0, -1/3)^{\mathrm{T}}, \\ p_1 = \left(-(\sqrt{3}/6)\mathrm{i}, 1/2, -(\sqrt{3}/6)\mathrm{i}\right)^{\mathrm{T}}, \end{cases}$$

which obviously satisfies $Aq_0 = A^{\mathrm{T}}p_0 = 0$, $Aq_1 = \mathrm{i}\omega_0 q_1$, and $A^{\mathrm{T}}p_1 = -\mathrm{i}\omega_0 p_1$, with the normalization conditions $\langle p_0, q_0\rangle = \langle p_1, q_1\rangle = 1$. The bilinear function $B(X,X)$ is

$$B(X,X) = 2\begin{pmatrix} xz \\ \eta z \\ -x^2 - \eta^2 - 2\eta z \end{pmatrix},$$

and the trilinear function $C(X,X,X)$ is

$$C(X,X,X) = 6\begin{pmatrix} 0 \\ 0 \\ x^2 z + \eta^2 z \end{pmatrix}.$$

Following the procedure mentioned above, we can obtain the values for the Poincaré normal coefficients:

$$\begin{cases} G_{200} = -(1/3), \\ H_{110} = -2/3 - (\sqrt{3}/3)\mathrm{i}, \\ G_{011} = 16/9, \\ G_{300} = -1/9, \\ G_{111} = -4/9, \\ H_{210} = (2\sqrt{3}/9)\mathrm{i}, \\ H_{021} = 1 + (89\sqrt{3}/243)\mathrm{i}. \end{cases}$$

Then, one gets the coefficients of the Gavrilov normal form: $B(0) = -1/3$, $C(0) = 16/9$ and $E(0) = 11/48$. Furthermore, we have

$$\begin{cases} s = \text{sign}(B(0)C(0)) = -1, \\ \theta(0) = \dfrac{\text{Re}(H_{110})}{B(0)} = 2 > 0. \end{cases} \tag{24}$$

In conclusion, when $a = 1, w = 1$, and $k = 1$, there is a fold-Hopf bifurcation point in system (2), and $s = -1, \theta(0) > 0$ indicate that a blow-up invariant tori appears near the fold-Hopf bifurcation point.

6.3. Numerical simulation

In this section, one further verifies the correctness of the Proposition 1 through numerical simulation. As shown in Fig. 8(a), at the fold-Hopf bifurcation point, the phase trajectory $\phi(X_0, t)$ converges to S_R, while $k = 0.99 \lessapprox 1$, an invariant torus is suddenly blow-up and $\phi(X_0, t)$ runs on it eventually. Two black closed curves on the x–z plane in Fig. 8(b) further show that system (2) is quasi-periodic. The red points approaching the black closed curves demonstrate that the motion of system (2) gradually reaches the invariant torus over time when $k = 0.99$.

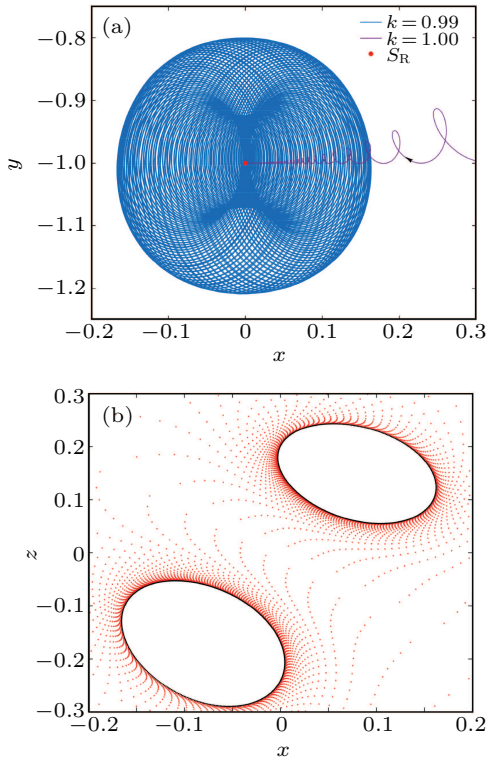


Fig. 8. Invariant torus of system (2) with the parameters $a = 1$, $\omega = 1$, $k = 0.99 \lessapprox 1$ and the initial conditions $X_0 = (0.5, 0.5, 0.5)$: (a) phase portrait on the x–y plane; and (b) Poincaré section on the x–z plane with $y = -1$.

7. Conclusion

In this paper, A class-B laser system with conservative and dissipative characteristics was studied. The study found that the numbers and stability of equilibrium points are affected by the system parameters. When $k = 0$, there are conservative flows in the class-B laser system. When $k \neq 0$, the conservative characteristics disappear and the dissipative characteristics become more and more obvious. Meanwhile, it is found that there are period, quasi-period, chaos, and coexisting attractors in system, these phenomena have been demonstrated by several numerical techniques including phase portraits, Poincaré sections, Lyapunov exponents, and other tools. In addition, through theoretical derivation, we find that the system has a fold-Hopf bifurcation and tori will "blow-up" at the bifurcation point, and the subsequent numerical simulations confirm the correctness of the theoretical derivation.

Acknowledgements

Project supported by the National Natural Science Foundation of China (Grant No. 61973175) and the Natural Science Foundation of Tianjin (Grant Nos. 20JCYBJC01060 and 20JCQNJC01450).

References

[1] Lorenz E N 1963 *J. Atmos. Sci.* **20** 130
[2] Matsumoto T 1984 *IEEE Trans. Circuits Syst.* **31** 1055
[3] Rössler O E 1976 *Phys. Lett. A* **57** 397
[4] Chen G R and Ueta T 1999 *Int. J. Bifurcat. Chaos* **9** 1465
[5] Wang F P and Wang F Q 2020 *Chin. Phys. B* **29** 058502
[6] Lei Y M and Zhang H X 2017 *Chin. Phys. B* **26** 030502
[7] Zhao C and Wu B 2021 *Chin. Phys. Lett.* **38** 030502
[8] Cang S J, Li Y, Kang Z J and Wang Z H 2020 *Chaos* **30** 033103
[9] Cang S J, Li Y, Xue W, Wang Z H and Chen Z Q 2020 *Nonlinear Dyn.* **99** 1699
[10] Li Y, Chen Z Q, Wang Z H and Cang S J 2021 *Int. J. Bifurcat. Chaos* **31** 2150198
[11] Dong E Z, Li R H and Du S Z 2021 *Chin. Phys. B* **30** 020505
[12] Qi G Y, Hu J B and Wang Z 2020 *Appl. Math. Model.* **78** 350
[13] Qi G Y 2019 *Appl. Math. Model.* **95** 2063
[14] Wang H B, Jiang W H and Ding Y T 2015 *Nonlinear Dyn.* **79** 2421
[15] Yamada T and Graham R 1980 *Phys. Rev. Lett.* **45** 1322
[16] Lugiato L A, Narducci L M, Bandy D K and Pennise C A 1983 *Opt. Commun.* **46** 64
[17] Arecchi F T, Lippi G L, Puccioni G P and Tredicce J R 1984 *Opt. Commun.* **51** 308
[18] Grigorieva E V and Kaschenko S A 2018 *Opt. Commun.* **407** 9
[19] Li Y Q 2014 *Appl. Math. Comput.* **226** 564
[20] Politi A, Oppo G L and Badii R 1986 *Phys. Rev. A* **33** 4055
[21] Oppo G L, Politi A, Lippi G L and Arecchi F T 1986 *Phys. Rev. A* **34** 4000
[22] Cang S J, Li Y, Kang Z J and Wang Z H 2020 *Chaos* **30** 033103
[23] Leonov G A, Kuznetsov N V and Vagaitsev V I 2011 *Phys. Lett. A* **375** 2230
[24] Guckenheimer J and Kuznetsov Y A 2007 *Scholarpedia* **2** 1855
[25] Kuznetsov Y A 2013 *Elements of applied bifurcation theory* (Germany: Springer Science & Business Media) p. 305